COMPOSITES & POLYCON 2009
American Composites Manufacturers Association
January 15-17, 2009
Tampa, FL USA

Strain Rate Effect and Size Effect on the Tensile Strength of z-reinforced p-aramid Fabric

Mr. Jacques W. Nader, Dr. Habib J. Dagher, and Mr. Fadi El Chiti
University of Maine

Mr. Stan Farrell and Mr. David Erb
Tex Tech Industries

Abstract

Previous research at the University of Maine and Tex-Tech industries has demonstrated the feasibility of using a 3-D hybrid fabric for ballistic protection [16]. The results of the 3-D hybrid fabric using 9 mm and 17 grain .22 FSP projectiles improved V-50 results over similar weight 2-D fabric by 9 to 13%. The material consists of multiple layers of woven ballistic fabric or cross laid tows, then covered with a layer of ballistic grade fiber felt. The fibers of the felt are then placed through the thickness using non-aggressive barbed needles. The through-thickness reinforcement appears to increase energy absorption of the layers by creating a large degree of fiber entanglement perpendicular to the woven fabric plane. The reinforcement also mechanically connects fabric plies which increases the area and the number of fibers that interact with the projectile. In this study, static and dynamic mechanical testing were conducted on the z-reinforced p-aramid fabric using a static then a high strain rate servo-hydraulic machine. The experimental test results were used to evaluate the strain rate effect and the size effect on the tensile properties of the z-reinforced p-aramid fabric. The findings enhance the understanding of the ballistic behavior, strain rate effects, and size effects of the 3-D hybrid p-aramid fabric. Resulting test data will be implemented in a 3-D ballistic finite element model to help predict ballistic properties of different types of z-reinforced p-aramid fabric materials.

Introduction

P-aramid fabric has been highly utilized in ballistic applications. The body armor currently used by US soldiers has more than 20 layers of fabric in addition to a ceramic insert. These body armors are heavy and cannot be used in areas were flexibility in the material is essential. The torso, neck and groin area cannot be protected with the current body armor and often these areas receive serious or fatal injuries for the soldier. A new fabric has been developed that utilized less layers of p-aramid fabric and is flexible enough to be used as body armor for the torso, neck and groin areas. In addition, the new fabric is purely made of p-aramid fabric and has a three dimensional structure. This unique three-dimensional structure performs exceptionally in catching and stopping fragments that approach at unpredictable angles and in various weights. Understanding the key parameters that attribute to this exceptional performance of the fabric has been a challenge to the manufacturers of the fabric. To understand these parameters and their effect on the overall ballistic performance of the fabric, both experimental test results and a finite element model will be used.

In general, most finite element modeling work uses mechanical properties obtained through quasi-static tests. However, the mechanical properties of most p-aramid fabric structures depend on the strain rate. Unfortunately reliable data on dynamic properties of p-aramid fabric are sparse because of the experimental difficulties associated with their determination. Moreover, most of the results are partial and do not permit implementation of a modeling approach with the entire set of material data.

Therefore, in this study, experimental testing will be conducted on 3-D hybrid p-aramid fabric using both quasi static and dynamic loading conditions, and the test results will be implemented in a non linear strain rate dependent finite element model to help predict ballistic properties of different types of z-reinforced p-aramid fabric materials.

3D hybrid ballistic fabric

The material consists of multiple layers of woven ballistic fabric or cross laid tows (Labeled as 1 in Figure 1). These fabric layers may consist of various weaves such as satin weaves or 0,90 unidirectional tows. The woven ballistic fabric is then covered with a layer of ballistic grade fiber felt (Labeled as 2 in Figure 1). The felt may be placed on one side, both sides, or within the fabric structure. Ballistic felts perform exceptionally well against fragments of exploding bombs and improvised explosive devices. Its success in catching and stopping fragments that approach at unpredictable angles and a variety of weight is due to the materials nonwoven structure that has fibers in a multitude of directions. The fibers of felt (batting) are then placed through the thickness (perpendicular to the x and y axis) using non-aggressive barbed needles (Labeled as 3 in Figure 1). The z-reinforcement appears to have three major benefits to increase the energy absorption of the fabric layers:

Through the infusion of z-directional reinforcement, a large number of fibers are entangled perpendicular to the woven fabric plane and mechanically connects the fabric plies. The mechanical bond prevents high-energy projectiles from spreading the individual tows of the fabric layers.

The infusion of the through-thickness fibers with the woven (x and y plane) ballistic fabric also inhibits delamination of individual layers. This z-directional reinforcement increases the area and number of fibers that interact with the projectile.

Through the addition of fibers in the z-direction, the density of the fabric is increased without increasing thickness. This forces the projectile to engage in a larger number of fibers per unit volume.

The specific objective of this study is to evaluate the size effect, strain rate effect, and punching density on the tensile strength of the 3-D hybrid ballistic p-aramid fabric. The overall objective of this work is to develop reliable mechanical properties to be implemented in a ballistic finite element model capable of properly predicting the ballistic behavior of the 3-D hybrid p-aramid fabric when subjected to high speed impact loading conditions.

Theory of size effect

It is very well known that there is a tendency for the strength of brittle materials to decrease with increasing specimen size [1-2-3]. This has major implications for the design of large composite structures or for obtaining reliable material properties to be implemented in any finite element modeling work. Previous research work has shown that the strength of basic glass, and carbon fibers used in most composites decreases with increasing the gage length of the specimens tested [4-5]. On the other hand, despite the importance of this subject there has been relatively little work performed to evaluate size effect on the mechanical properties of the 3D hybrid p-aramid fabric.

The decrease in strength with the increase in specimen size may be explained using the Weibull strength theory [6]. This theory assumes that the strength of a brittle material is controlled by the statistical distribution of the flaws. The probability of survival, P(s), under a stress or strain fields s is defined by:

$$P(s) = \exp\left[-\int_V \left(\frac{s}{s_0} \right)^m dV \right] \qquad (1)$$

Where s_0 is the characteristic strength which may be expressed in terms of either stress or strain to failure and m is the Weibull modulus or shape parameter. An assumption is made that the values of the shape parameters s_0 and m are material constants.

For two tests of different size specimens with an equal probability of survival, equation (1) gives:

$$\int_{V0_1} {s_0}^m \, dV = \int_V s^m \, dV \qquad (2)$$

Normalizing the stress field in terms of the maximum stress, $\bar{s}$, and a position function, A , gives:

$$s = \bar{s}\, A(x, y, z) \qquad (3)$$

Substituting into equation (2)

$$\bar{s}_0^m \int_{V_0} A^m \, dV = \bar{s}^m \int_V A^m \, dV \qquad (4)$$

For identically scaled specimens, with the same stress distributions, the functions A are equivalent, and equation (4) becomes:

$$\bar{s}_0^m \, V_0 = \bar{s}^m \, V \qquad (5)$$

This leads to

$$\bar{S} = \bar{S}_0 \left(\frac{V_0}{V} \right)^{1/m} \qquad (6)$$

For a given set of specimen with the same width and thickness, equation (6) reduces to:

$$\bar{S} = \bar{S}_0 \left(\frac{L_0}{L} \right)^{1/m} \qquad (7)$$

Therefore the strength ratio of two different size specimens depends on the relative length ratio and the Weibull parameter m. The Weibull parameter is a measure of the amount of scatter in the specimen length. As m decreases, the amount of scatter in the material length increases which results in a greater size effect.

Material used in the experimental work

Two types of experiments (quasi static and dynamic tension tests) were completed with different experimental techniques. The tests were conducted using different fabric types having different z-fiber reinforcement densities. The density of z-fiber reinforcement was measured according to the number of needle penetrations per square inch applied on the fabric during manufacturing. Six types of densities were tested:

300 PSI, 500 PSI, 800 PSI, 1200 PSI, 1600 PSI, and 2400 PSI (note that PSI designates Penetrations per square inch). The fabric was made of 4 layers of fabrics and 1 layer of felt on top. Each layer of fabric is 8 H Satin Weave Twaron® (~840 denier) 5.15 oz/yd2 (174.61 g/m^2) and the felt is 2.5 oz/yd^2 (84.76 g/m^2) Twaron® felt.

Experimental procedure for size effect study on tensile strength

Tensile tests were performed according to ASTM D5035 testing method [7] on six sets of eight specimens each. Each set had a different z-reinforcement density. Six types of densities were tested: 300 PSI, 500 PSI, 800 PSI, 1200 PSI, 1600 PSI, and 2400 PSI. All specimens had a rectangular shape with a width equals to 1in. Seven different gage lengths were used: 0.5" (12.7 mm), 1" (25.4 mm), 2" (50.8 mm), 3" (76.2 mm), 5" (127 mm), and 7"(177.8 mm) to evaluate the effect of gage length on the tensile strength of the 3-D p-aramid hybrid fabric. The tests were conducted using an Instron servo-hydraulic testing machine equipped with tensile fixtures at a strain rate below 1s^{-1}. Most test specimens failed in tension in the gage length.

Test results showed a significant decrease in the tensile strength when increasing the gage length of the test specimens for all types of fabric, as shown in Figure 2. It was not surprising to see that the 3-D hybrid p-aramid fabric exhibits significant size effect which can be explained by the punching in the z-direction which damages the fibers in the longitudinal direction and therefore increased the scattered flaws along the length of the specimen.

These observations will be critical and useful to develop reliable ballistic finite element models that accounts for the fabric type and the size effects.

Experimental data fit with the Weibull size effect theory

The experimental test results were used to calculate the Weibull parameter m as defined by equation 7, and demonstrate the ability of the Weibull model to fit the data. The stress field of the tension specimens is assumed constant over the gage length. A plot of the natural log of the gage length versus the natural log of the ultimate strength is shown in figure 3 with the least square linear Weibul fit curves for each type of fabric. Figure 3 indicates a good correlation between the Weibull least square fit curves and the experimental data.

The Weibull parameter m for each material type was computed by calculating the negatives of the slopes of the lines in Figure 3. A summary of the Weibull parameters and the R^2 values of the linear fit curves is presented in Table 1. The values of m were equal to 3.4, 2.14, 2.11, 1.83, 1.44 and 1.4, corresponding to the 300 PSI, 500 PSI, 800 PSI, 1200 PSI, 1600 PSI, and 2400 PSI fabrics, respectively. It is interesting to see that the Weibull parameters constantly decreases as the punch density increases and that the highest Weibull parameter corresponded to the fabric with the lowest punching density, indicating less scatter in the material and less size effects. On the other hand, the lowest Weibull parameter corresponded to the fabric with the highest punching density, indicating high scatter in the material and higher size effects. These results were expected since the fabric with higher punching density has much more damaged fabric in the longitudinal direction which increases the amount of scattered flaws along the specimen length

It was also interesting to compare the percent decrease in the ultimate strength when testing a 7" (177.8 mm) gage length specimen versus a 0.5"(12.7 mm) gage length specimen. The results show a 63.8 %, 68.7%, 78.9%, 79.7%, and 81% decrease in the ultimate strength for the 300 PSI, 500 PSI, 800 PSI, 1200 PSI, 1600 PSI, and 2400 PSI, respectively. These results illustrate the fact that the materials with higher punch density exhibit higher size dependence than the material with lower punch density.

Punch density effect on tensile properties under quasi static loading conditions

Another key parameter to be investigated in this study is the effect of the punching density on the ultimate strength of the 3-D hybrid p-aramid fabric. Figure 4 shows the decrease in the tensile strength of the 3D hybrid fabric as a function of the Punching density for the 0.5" (12.7 mm), 1" (25.4 mm), 2" (50.8 mm), 3" (76.2 mm), 5" (127 mm), and 7"(177.8 mm) gage length specimens tested at a strain rate below 1s^{-1}. This decrease in strength is due to the increase in the number of broken fibers in the longitudinal direction cause by the z-reinforcement.

A linear square fit curve was used to represent the experimental data, as shown in Figure 4. It is interesting to observe that the linear least square curves correlate well with the experimental test results for all specimen sizes. This means that the ultimate strength of the 3-D hybrid p-aramid varies linearly with the punching density in the z-direction for all specimens. The slopes of the linear fit curve were -391, -385, -406, -380, -297, and -259 for the 300 PSI, 500 PSI, 800 PSI, 1200 PSI, 1600 PSI, and 2400 PSI fabric, respectively. This indicates that the fabrics with different gage length exhibit different behavior when changing the punching density as discussed in the previous section.

Theory of strain rate effect

P-aramid fabric material is widely used to produce personnel protection systems because of their impactresistant properties. This type of material is subjected to high strain rate loading when the projectile hits the fabric. Therefore in order to accurately understand the ballistic behavior of the fabric during impact, many aspects of fabrics including material properties need to be studied under dynamic loading conditions. Currently, few general laws from the literature describe the changes in the mechanical properties of p-aramid fabric as a function of the strain rate [8]. In his study, Yang et al., studied the rate dependence of Kevlar® fiber strength based on a bimodal Weibull distribution statistical model of strain rate dependence of fibers and determined the mechanical properties and Weibull parameters of fibers from bundle tests. In this study, we will evaluate the strain rate effect on the tensile strength of the 3-D hybrid p-aramid fabric and try to verify the applicability of the bimodal Weibull distribution statistical constitutive model on the 3-D reinforced p-aramid fabric using experimental test results.

The increase in strength with increasing the strain rate may be explained using the bimodal Weibull distribution statistical model of strain rate dependence which can be summarized as follow:

$$S = S_0[1 + C\ln(\dot{\varepsilon}/\dot{\varepsilon}_0)] \qquad (8)$$

Where $\dot{\varepsilon}_0$ is the reference strain rate, and S_0 is the ultimate strength measured at the reference strain rate $\dot{\varepsilon}_0$. S is the ultimate strength measured at the strain rate $\dot{\varepsilon}$ and C is called rate sensitivity coefficient.

Therefore the strength ratio of two identical specimens tested at two different strain rates depends on the relative strain rate ratio and the rate sensitivity coefficient C. The rate sensitivity coefficient C is a measure of the material rate dependence, and is considered a material property. In this case, as the value of C increases, the strain rate dependence increases for a given type of materials.

Experimental procedure for strain rate effect study on tensile strength

The use of servo-hydraulic testing machines to conduct compression and tension testing at medium strain rates (1-100 s^{-1}) is very well documented in the literature [9-15]. In this study, dynamic tensile tests were conducted using a high rate INSTRON servo-hydraulic testing machine. The machine can reach a speed of 65.6ft/s (20m/s), with a load capacity of 2250 lbs (100KN).

The dynamic tensile tests were conducted on six sets of eight specimens each. Each set have a different z-fiber reinforcement density. Six types of densities were tested: 300 PSI, 500 PSI, 800 PSI, 1200 PSI, 1600 PSI, and 2400 PSI. All specimens were cut and tested according to the ASTM D5035 tension test method. All specimens had a rectangular shape with a width equals to 1" (25.4 mm) and a gage length equals to 3" (76.2 mm). The specimens were loaded at three loading speeds: 6.6 ft/s (2m/s), 16.4 ft/s (5m/s), and 21.32 ft/s (6.5m/s) resulting in loading rates of $26s^{-1}$, $66s^{-1}$, and $85s^{-1}$, respectively. The average value of the tensile strength was recorded for each tested set.

Experimental data fit with the bimodal Weibull statistical model of strain rate effect

The dynamic test results showed that the tensile strength increases when increasing the loading rate for all types of fabric, as shown in Figure 5. A summary of the experimental test results is shown in Table 4. To better understand the strain rate effect on the tensile strength on the basis of Weibull theory, the tensile strength was plotted as function of $\ln(\dot{\varepsilon})$, as shown in Figure 6. The relationship between S_{max} and $\ln(\dot{\varepsilon})$ is approximately linear in the range of 26 – 85/s. A summary of the linear least square fit equations is given in Table 2 for all types of fabric.

In order to quantify the strain rate sensitivity for all types of fabric, the sensitivity coefficient must be computed.

Therefore, the ultimate strength values were plotted as functions of $\ln(\dot{\varepsilon}/\dot{\varepsilon}_0)$, with $\dot{\varepsilon}_0$=26/s for all types of fabric. Figure 7 shows the linear square fit curves for these plots for all types of fabric tested between 26 and 85/s and a summary of the values of C and S_0 is given in Table 3. It was interesting to see that the values of C increased when increasing the punching density from 300PSI to 1600PSI. This behavior can be explained by the increased number of entangled fibers perpendicular to the woven fabric plane which mechanically connects the fabric plies when loaded at high speed. These connections behave more effectively when the specimen is loaded at high rates. In general, the higher the loading rate is, the stronger these connections are.

On the other hand it was interesting to see that the strain rate sensitivity coefficient C for the 2400PSI fabric is low, indicating a low strain rate effect. In this case, even though the 2400 PSI fabric has a high number of entangled fibers, the number of damaged fibers in the longitudinal direction might be very high causing a decrease in the effectiveness of the mechanical connections caused by the z-reinforcement. These observations will be useful to better understand the ballistic behavior of different types of fabric and to find a correlation between mechanical properties and ballistic behavior.

Punch density effect on the tensile strength at high strain rates

The effect of the z-direction punching density on the tensile strength of the 3-D reinforced p-aramid fabric was studied at different strain rates. The ultimate strength values of the tested specimens were plotted as functions of the punching densities in the z-direction. Binomial best fit curves were used to simulate the experimental results, as shown in Figure 8. The experimental test results showed that at all loading rates, the ultimate strength decreases when increasing the punching density in the z-direction.

It is also interesting to note that the effect of the z-reinforcement on the tensile strength changes with the loading rate. This behavior is illustrated by the change in the shape of the best fit curves from a concave up curves for the $0.001s^{-1}$ and the $26s^{-1}$ loading rates to a concave down curves for the $66s^{-1}$ and $85s^{-1}$ loading rates. This means that at low strain rates, the ultimate strength of the fabric is very sensitive to the z-reinforcement when going from 300PSI to 1600PSI, and this effect decreases after 1600PSI. On the other hand, when testing at $66s^{-1}$ and $85s^{-1}$, the ultimate strength of the fabric is less sensitive to the z-reinforcement when going from 300PSI to 1200PSI and is very sensitive when going from 1600 PSI to 2400 PSI. These observations are critical in understanding the ballistic behavior of 3-D hybrid p-aramid fabric with different z-reinforcement densities.

Conclusion

In this study both experimental testing and mathematical modeling where used to better understand the dependence of the 3-D hybrid p-aramid fabric on the punching density, specimen size, and loading rate.

In the experimental work, specimens with different dimensions and z-reinforcement densities were tested under both quasi static and dynamic loading conditions. The test results showed that the 3-D hybrid p-aramid fabric exhibits a significant size effect. All specimens showed a decrease in the ultimate strength when increasing the specimen length. This behavior can be explained by the increase in the number of broken fibers in the longitudinal direction caused by the z-reinforcement, causing an increase in the amount of scattered flaws along the length of the material. The Weibull size effect theory was used to quantify the size effect on the ultimate strength. The Weibull parameters were calculated for each material type and showed great correlation with experimental test results.

On the other hand, the 3-D hybrid p-aramid fabric showed a significant strain rate effect. In general, all specimens showed an increase in the ultimate strength when increasing the loading rate. This behavior was explained using the bimodal Weibull strain rate effect theory which successfully predicted this behavior. The strain rate sensitivity coefficient were calculated for all material types and showed good correlation with experimental test results.

Finally, the experimental test results and the observations presented in this study will be implemented in a non linear strain rate dependent ballistic finite element model to properly predict the ballistic behavior of the 3-D hybrid p-aramid fabric when subjected to different loading conditions and help optimize the design of z-reinforced p-aramid fabrics ballistic structure for optimum ballistic behavior.

Acknowledgments:

We hereby acknowledge support for the technical effort by the United States Army under a Small Business Technical Transfer Research (STTR) Program. Dr. Bruce LaMattina was the Government Project Engineer. The content and information does not necessarily reflect the position of the United States Army.

Also, the authors would like to thank General Motors Corporation for generously allowing the use of their high strain rate testing machine for the dynamic testing.

References:

1. Z. P. Bazant. Size effects. International Journal of Solids and Structures, 37, 69 (2000)

2. T. Okabe, N. Takeda, Size effect on the tensile strength of unidirectional CFRP composites- experiment and simulation, Composite Sciences and Technology, 62, 2053 (2002)

3. M.R. Winsom. Size effects in the testing of fiber-composite materials. Composite Science Technology, 59, 1937 (1999)

4. A.G. Metcalfe, G. K. Schmitz. Effect of length on the strength of glass fibers. American Society for Testing Materials, (1964)

5. M. G. Bader, A. M Priest. Statistical aspects of fiber and bundle strength in hybrid composites. Proceedings of the 4th international on Composite Materials, Tokyo, 1, 1129 (1982)

6. W. Weibull. A statistical distribution function of wide probability. Journal of Applied Mechanics, l18, 293 (1951).

7. ASTM Standard D5035, 2006, Standard Test Method for breaking strength ad elongation of textile Fabrics, ASTM International, West Conshohocken, PA, www.astm.org

8. Yang Wang, and Yuanming Xia, The effects of strain rate on the mechanical behavior of Kevlar® fiber bundles: an experimental and theoretical study, Composites Part A, 1411 (1998)

9. X.Xiao, Dynamic tensile testing of plastic materials, Polymer Testing. Polymer testing, (2007)

10. P.C.Bastias, S.M. Kulkarni, K.Y.Kim, J.Gargas, Non-contacting strain measurements during tensile tests, Exp. Mech. 78, 78 (1996)

11. D.M.Bruce, D.K. Matlock, J.G Speer, A.K. De, Assessement of the material strain rate dependent of automotive sheet steels, SAE, 10, 507 (2004)

12. S. Hill, P. Sjoblom, Practical considerations in determining high strain rate, Mater. Prop., SAE 981136.

13. J. Fitoussi, F. Meraghni, Z. Jendli, G. Hug, D. Baptiste, Experimental methodology for high strain rates tensile behavior analysis of polymer matrix composites, Compos. Sci. Technol. 65, 2174 (2005)

14. Garg S. K Savalbonas V. and Gurtman. G A, Analysis of structural composite materials, Marcel Dekker, 1, 201 (1973)

15. C.S.Chou, K.D. Robertson, J.H.Rainey, The effect of strain rate and heat developed during deformation on the stress strain curve of Plastics, Exp. Mech. 13, 422 (1973)

16. United States Patent 7101818, European Patent EP1579167

Tables:

Table-1

Fabric Type	R^2	m (weibull parameter)
300 PSI	0.943	3.4
500PSI	0.946	2.14
800PSI	0.971	2.11
1200PSI	0.945	1.83
1600PSI	0.965	1.44
2400PSI	0.976	1.4

Table-2

Fabric Type	Weibull Least square fit
300 PSI	$1144.9 \ln(\dot{\varepsilon}) - 1317.3$
500PSI	$1679.5 \ln(\dot{\varepsilon}) - 3526.3$
800PSI	$1687.5 \ln(\dot{\varepsilon}) - 3793.6$
1200PSI	$1925.4 \ln(\dot{\varepsilon}) - 5005.3$
1600PSI	$1984 \ln(\dot{\varepsilon}) - 5501.4$
2400PSI	$809.34 \ln(\dot{\varepsilon}) - 1773.6$

Table-3

Fabric Type	Weibull Least square fit of S/S_0	C	R^2	S_0
300 PSI	$1+ 0.47\ln(\dot{\varepsilon}/\dot{\varepsilon}_0)$	0.47	0.99	2423.6
500PSI	$1+ 0.856\ln(\dot{\varepsilon}/\dot{\varepsilon}_0)$	0.856	0.98	1961.4
800PSI	$1+ 0.98\ln(\dot{\varepsilon}/\dot{\varepsilon}_0)$	0.98	0.99	1720.5
1200PSI	$1+ 1.497\ln(\dot{\varepsilon}/\dot{\varepsilon}_0)$	1.497	0.99	1285.9
1600PSI	$1+ 2.02\ln(\dot{\varepsilon}/\dot{\varepsilon}_0)$	2.02	0.99	981.34
2400PSI	$1+ 0.93\ln(\dot{\varepsilon}/\dot{\varepsilon}_0)$	0.93	0.99	870.96

Table-4

Max load lbs-(N)	Punch Density (PSI)					
Strain Rate s^{-1}	**300**	**500**	**800**	**1200**	**1600**	**2400**
<0.001	2312 (10284)	1785 (7940)	1332 (5925)	1132 (5035)	665 (2958)	360 (1601)
26	2417 (10751)	1922 (8549)	1702 (7571)	1260 (5640)	959 (4266)	880 (3914)
66	3502 (15577)	3674 (16342)	3351 (14906)	3165 (14078)	2899 (12895)	1573 (6997)
85	3750 (16681)	3805 (16925)	3644 (16209)	3466 (15417)	3242 (14421)	1856 (8256)

Figures:

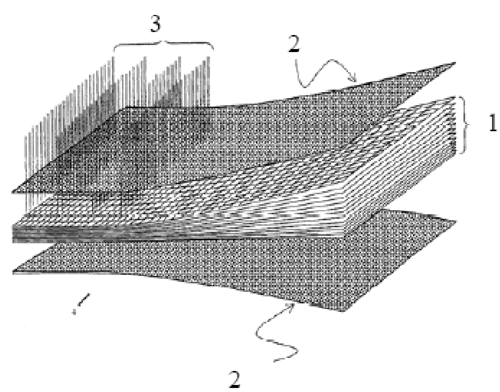

Figure 1: Schematic of Text Tech Industry's Ballistic Fabric Technology

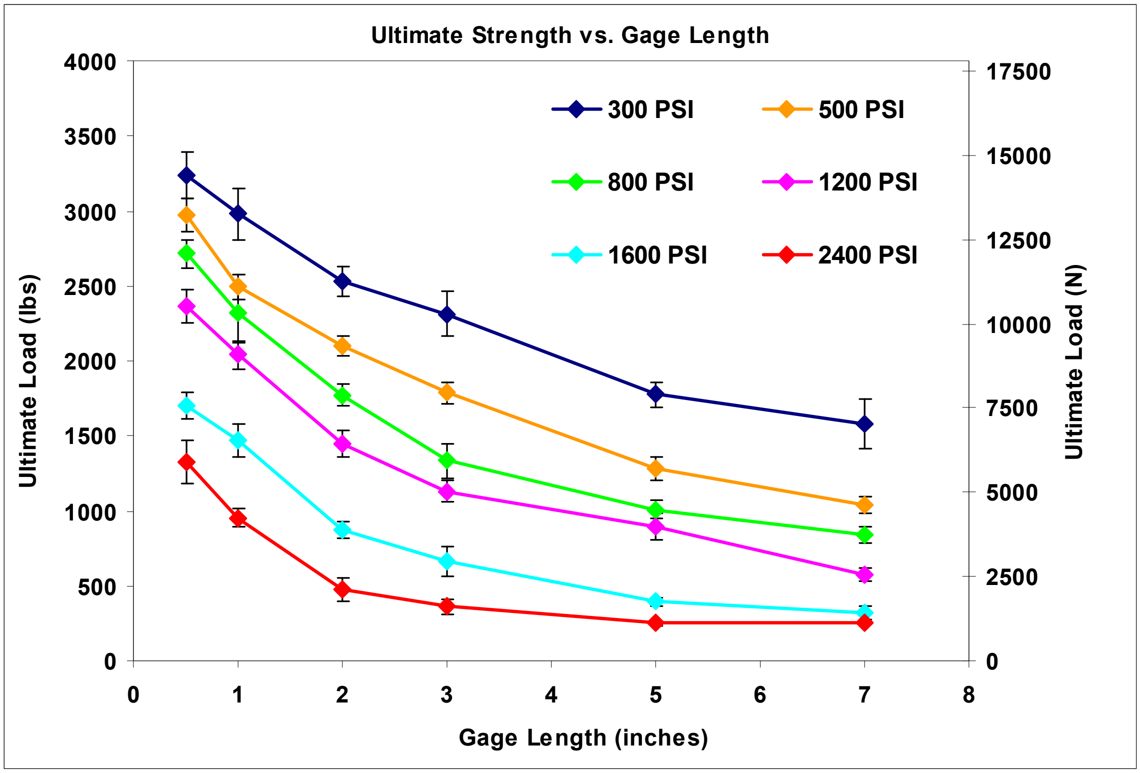

Figure 2: Ultimate Strength vs. Gage length for fabrics with different z-reinforcement densities

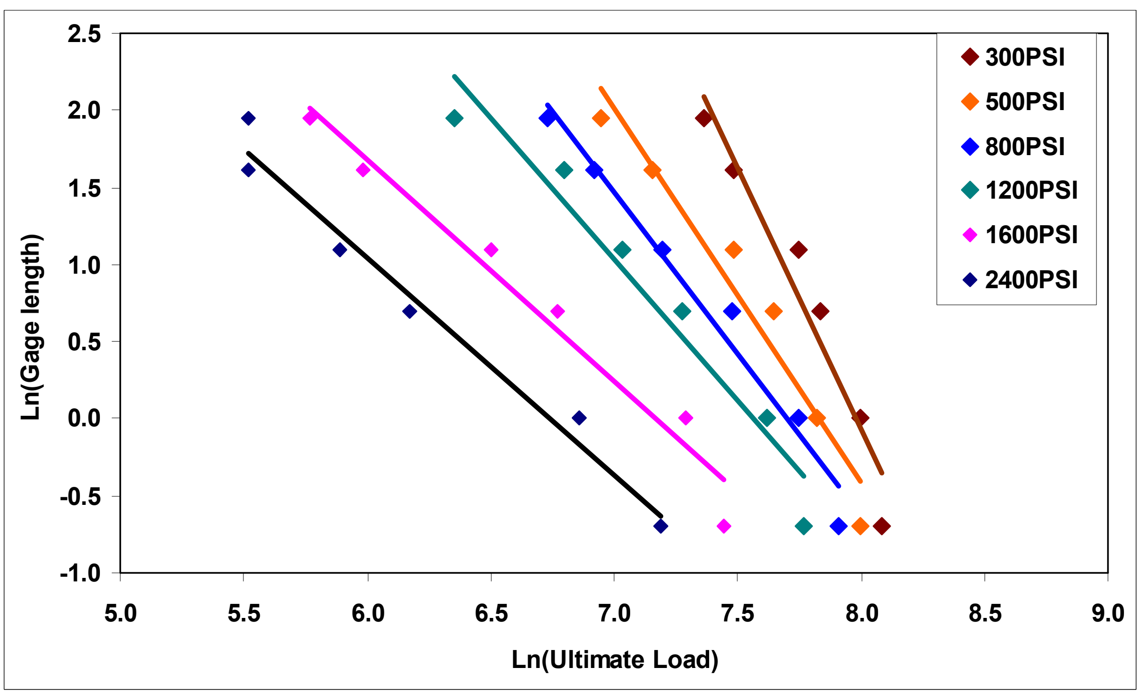

Figure 3: Weibull least squares fit to experimental data

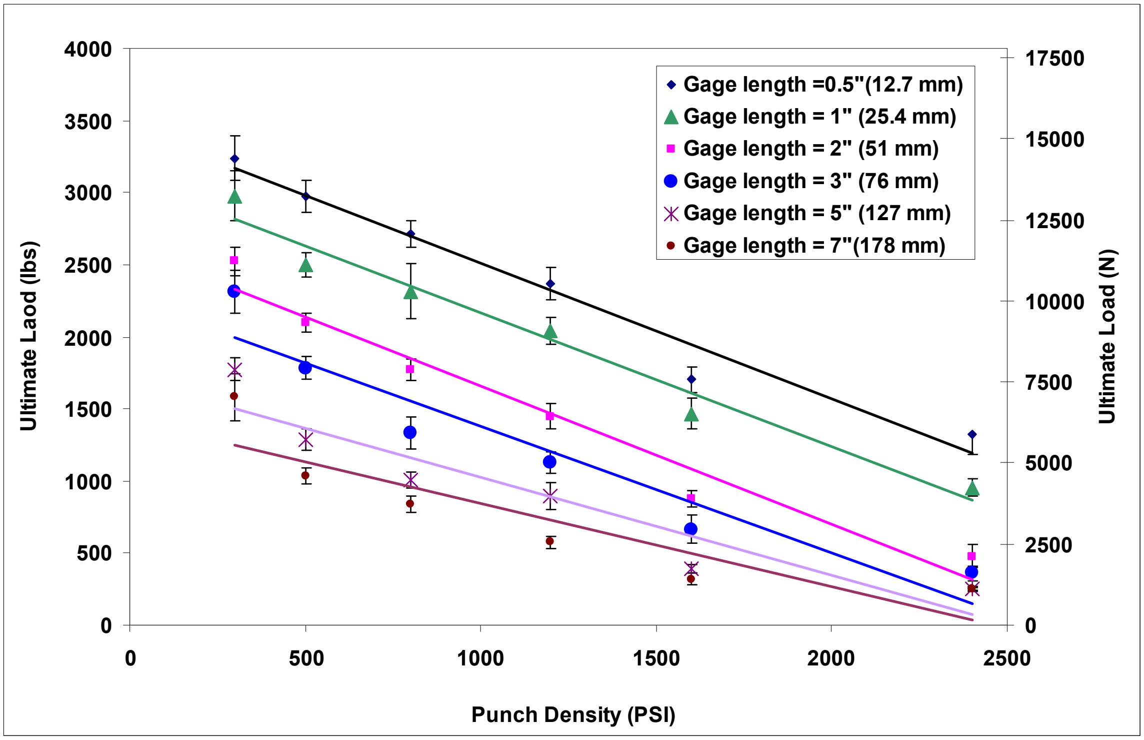

Figure 4: Ultimate Load vs. Punch density with a linear least square fit of the experimental results

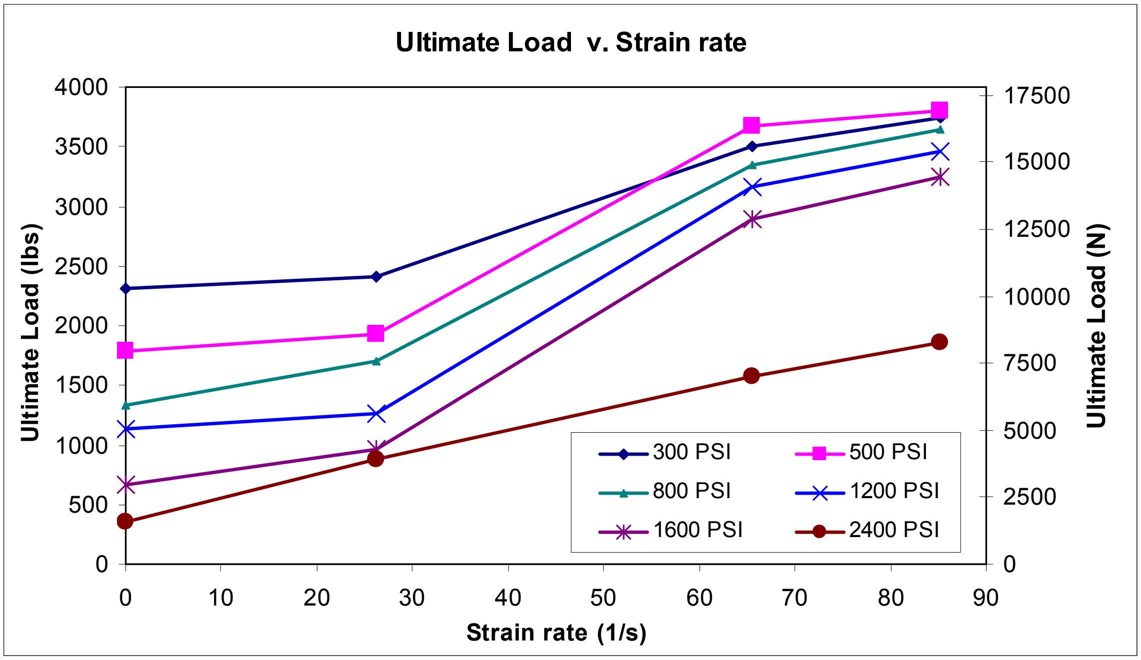

Figure 5: Ultimate Load vs. strain rate for all types of fabric

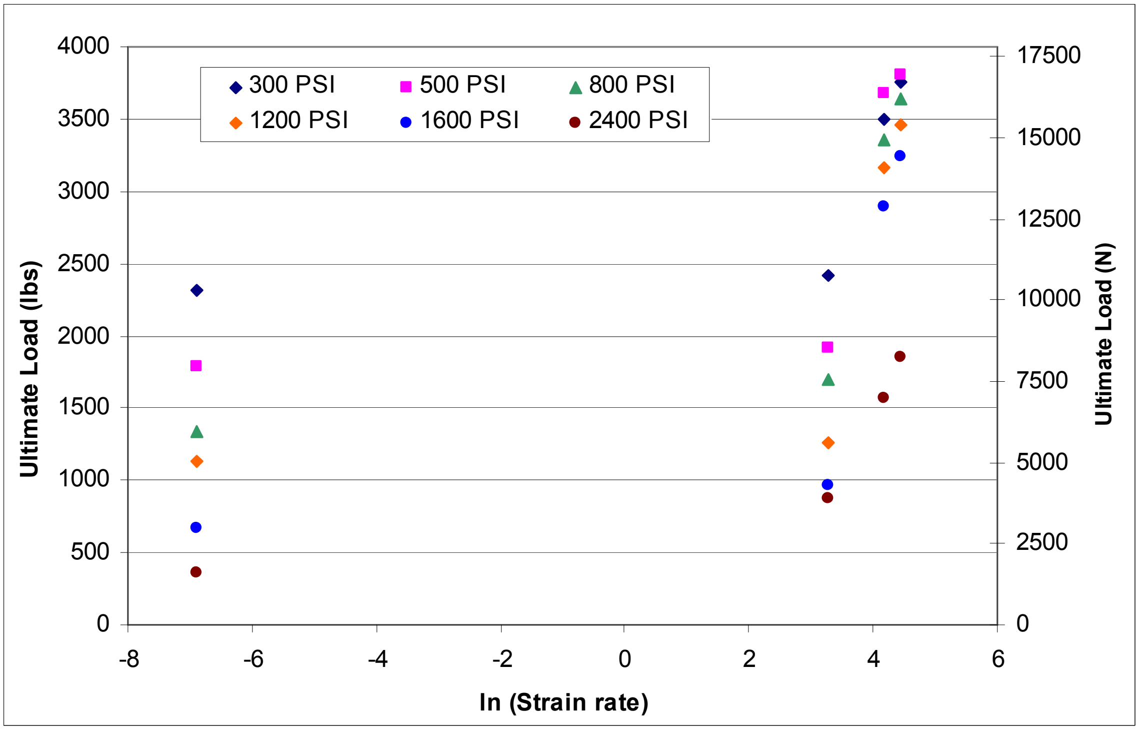

Figure 6: Ultimate Load vs. Ln(Strain rate) for the 3” (76.2 mm) gage length specimens

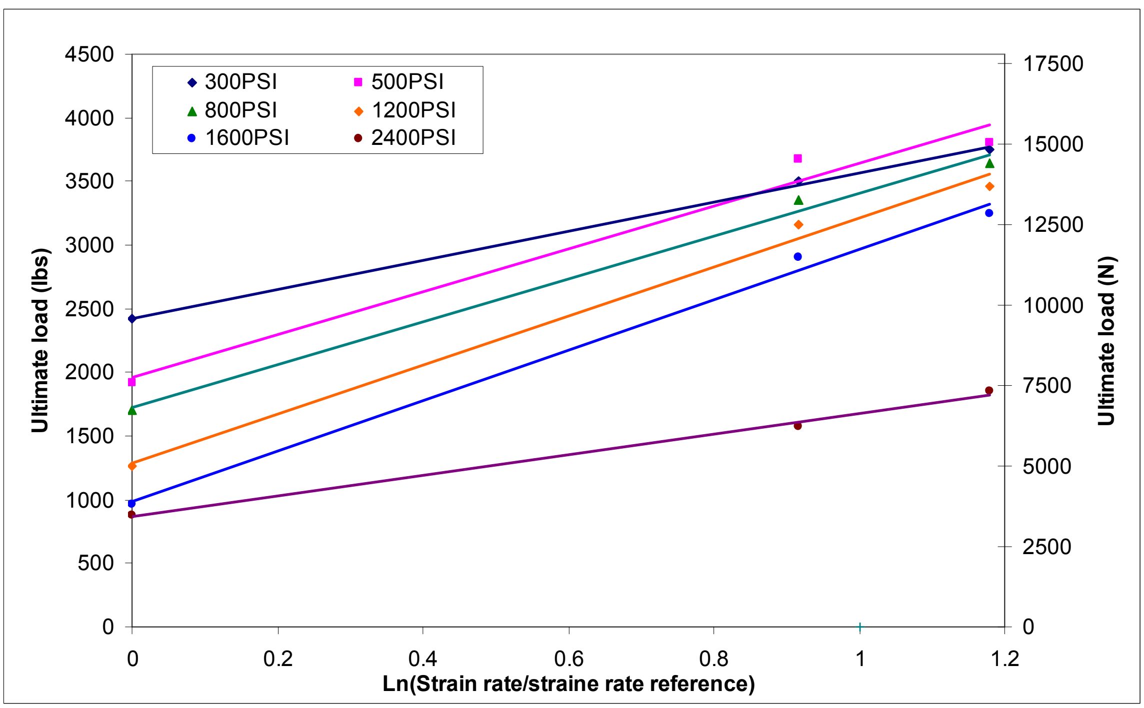

Figure 7: Strength vs. Ln(strain rate) for 3" (76.2 mm) gage length specimens with linear square fit of the experimental results

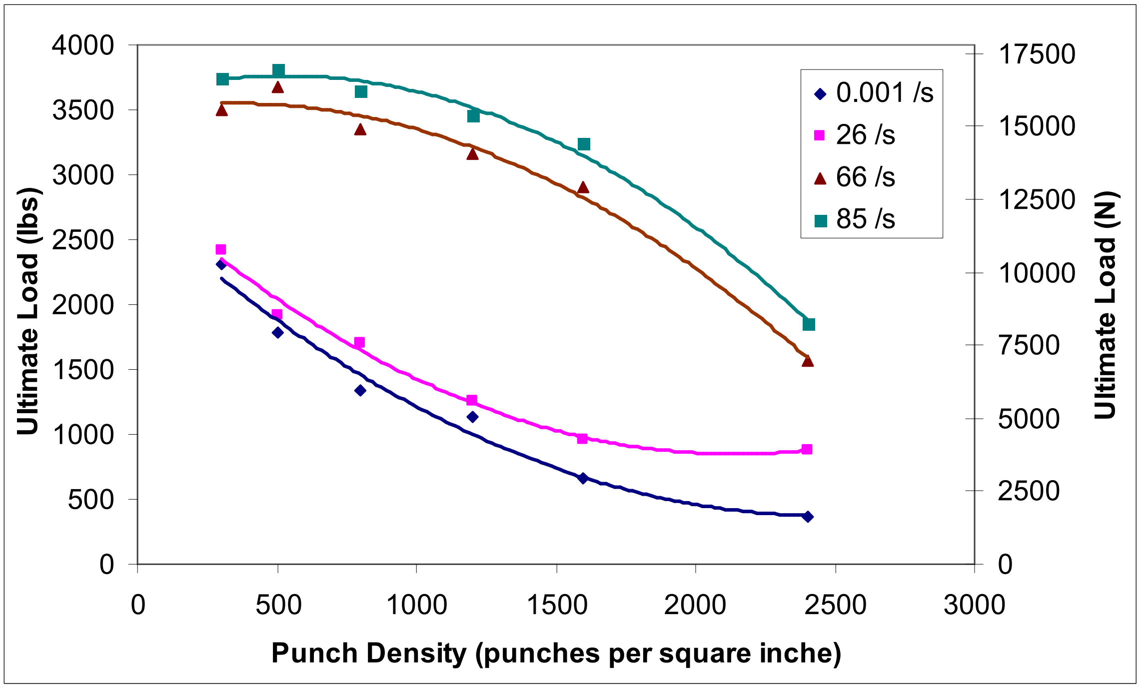

Figure 8: Ultimate Load vs. Punch density for the 3" (76.2 mm) gage length specimens with a polynomial curve fit of the experimental results